Available online at www.sciencedirect.com
ScienceDirect
Polymer 48 (2007) 4438–4448
polymer
www.elsevier.com/locate/polymer

Fabrication and characterization of fullerene–Nafion composite membranes

Ken Tasaki*, Jeffrey Gasa, Hengbin Wang, Ryan DeSousa

MC Research and Innovation Center, 601 Pine Avenue, Goleta, CA 93117, USA

Received 23 December 2006; received in revised form 13 May 2007; accepted 15 May 2007
Available online 25 May 2007

Abstract

Fullerene–Nafion composite membranes have been fabricated through a new solution casting for the first time. The fullerenes used for the composites included C_{60} and polyhydroxy fullerene (PHF), $C_{60}(OH)_n$ ($n \sim 12$). The dispersion of the fullerene in the composite membrane was much more refined with smaller agglomeration particles, relative to the previously prepared fullerene–Nafion composites in which the fullerene was introduced through doping. The miscibility of the hydrophobic fullerene, C_{60}, in the Nafion matrix was further improved by a new fullerene dispersant, poly[tri(ethylene oxide)benzyl]fullerene, $C_{60}[CH_2C_6H_4(OCH_2CH_2O)_3OCH_3]_n$ ($n \sim 5$), synthesized in this work. The solution-cast fullerene composites also demonstrated a significant improvement in the physical stability relative to the fullerene-doped Nafion composites through a better integration of the fullerene into the Nafion matrix. Furthermore, increased loadings of the fullerene in Nafion were made possible through the new solution-casting method, compared to the previous doping method. The water characteristics in the fullerene composites have been examined by TGA and ^1H pulse NMR measurements. The interactions between the fullerene and the Nafion have been studied through ATR FT-IR and molecular dynamics simulations which suggested PHF resides primarily in the hydrophobic domain of Nafion when the loading was low. The voltammetric measurements also have shown that the fullerene composites have the reduced limiting current density, compared to Nafion membranes without fullerenes.
© 2007 Elsevier Ltd. All rights reserved.

Keywords: Fullerene composites; Membrane fabrication; Water characteristics

1. Introduction

Fullerenes possess unique characteristics such as the high electron affinity [1], the high volumetric density of the functional groups [2], radical scavenging [3], the improved thermal and mechanical stabilities of polymers [4–6], the enhanced gas selectivity of polymers [7], and others. Yet, the fact that fullerenes are powders has hindered practical applications of their unique properties. Incorporation of fullerenes into polymeric materials to improve their processability has become a common practice for practical applications of fullerenes in areas such as optelectronics, photovoltaics, optics, fuel cell membranes, and life science [8–13]. Chemical functionalization of fullerenes is often performed, for example, to increase the miscibility of fullerenes with host polymers [14,15]. Yet, chemical attachment of fullerenes to a polymer is not always straightforward, despite a number of fullerene-attached polymers which have been successfully synthesized in the past [16]. Also, chemical functionalization may affect the unique nature of C_{60} itself. On the other hand, there have been a number of examples for fabrication of fullerene composites with polymeric materials [11,17–24]. Among others, fullerene–Nafion composite films have promising potentials in applications such as electrocatalysis [22], fuel cells [2], and optics [10,19].

One of the first attempts to fabricate a C_{60}–Nafion composite film was made by Guo et al., who soaked a Nafion membrane in a saturated methanol solution of a series of methanofullerene derivatives having hydrocarbon chains terminated by ethylene oxide units [19]. The mixing of the fullerene derivative in Nafion was achieved by a diffusion of the fullerene derivative

* Corresponding author: Tel./fax: +1 310 373 4196.
E-mail address: ken_tasaki@m-chem.com (K. Tasaki).

0032-3861/$ - see front matter © 2007 Elsevier Ltd. All rights reserved.
doi:10.1016/j.polymer.2007.05.049

through the Nafion matrix [19]. Though the dispersion of the fullerene derivative was reported to be uniform with the average agglomeration particle size of 5 nm, it was not clear how much of the fullerene was incorporated into the Nafion membrane through this "doping". Furthermore, the applicability of this doping process depends strongly on the interactions between the fullerene derivative and the Nafion. In fact, incorporation of either C_{60} or hydrophobic peripheral chain-attached C_{60} into Nafion film was not observed by this particular method [23]. Nor was controlling the amount of the fullerene incorporated into Nafion straightforward through the doping. The diffusion-based process also requires long preparation time, e.g., several days just for the soaking of the Nafion film [19]. Melt blending is another method by which a fullerene can be incorporated into a polymer, especially when the two components are immiscible [6]. Still, a possibly significant morphological change in the polymer during the melt processing raises a concern, along with destruction through compounding and extrusion of the polymer.

Improved fabrication methods for incorporation of fullerenes into polymeric materials will continue to benefit the use of fullerenes in a variety of existing as well as new applications. In particular, solution-casting methods may provide more flexibility in types of fullerenes used, controlling the dispersion, and the loading in a polymer than doping methods. They also present a less distractive means, compared to doping or melt blending. Yet, fullerene derivatives tend to aggregate in solution as well as in polymeric materials. Thus, solution casting of fullerene–polymer composites often poses a challenge, depending on the fullerene and the host polymer. Incorporation of C_{60} into Nafion, for example, has been only reported by doping which differs from that used in Ref. [23] [2]. Polyhydroxy fullerene (PHF), $C_{60}(OH)_n$ ($n \sim 12$), is another interesting fullerene in that it has an extremely high volumetric density of functional groups, approximately 12 hydroxy groups in a cavity of about 1 nm in diameter, a size of C_{60}. Its strong hygroscopic characteristic has been found recently [2]. Incorporation of neither C_{60} nor PHF into Nafion membrane through solution casting has been reported. In this report, we present a new membrane fabrication of the C_{60}–Nafion and the PHF–Nafion composites and their characterization. We also synthesized a new fullerene dispersant, poly[tri(ethylene oxide)benzyl]fullerene (to be denoted as $C_{60}(TEO)_n$), to improve the dispersion of extremely hydrophobic C_{60} in the microphase-separated Nafion mixed with both hydrophilic and hydrophobic domains and demonstrate its effectiveness. As one of the possible applications of the fullerene composite membranes prepared in this study, we fabricated a membrane–electrode assembly for direct methanol fuel cell and measured the limiting current density of the fullerene composites and their proton conductivity.

2. Experimental

2.1. Synthesis of fullerene derivatives

C_{60} was purchased from SES Research, Houston, TX. PHF was synthesized according to Chiang et al., [25] through sulfonation of C_{60} and the subsequent hydrolysis. The synthesis of $C_{60}(TEO)_5$ was based on the atom transfer radical addition (ATRA) reaction in four steps to attach multiple ethylene oxide chains to C_{60}, as illustrated in Fig. 1. In a typical ATRA step, C_{60} (720 mg, 1 mmol), tri-ethylene oxide benzyl bromide (8 mmol) and bipyridine (1.56 g, 10 mmol) were dissolved in 100 ml *ortho*-dichlorobenzene (ODCB). The solution was degassed for 10 min and CuBr (0.789 g, 8 mmol) was added quickly. The vessel was sealed and heated at 110 °C for 2 days until a green precipitation occurred. H_2S was bubbled through the solution to completely precipitate the Cu residue, then the solution was filtrated and ODCB was removed under vacuum. The details of the characterization have been reported elsewhere [26].

2.2. Preparation of membranes

The fullerene-doped Nafion composites (denoted as C_{60}/Nafion 117 or PHF/Nafion 117) were prepared as they were in the previous method [2]. The preparation of the solution-cast fullerene–Nafion composites was as follows: a 5% Nafion dispersion, purchased from Alpha Aesar, was dried at 80 °C

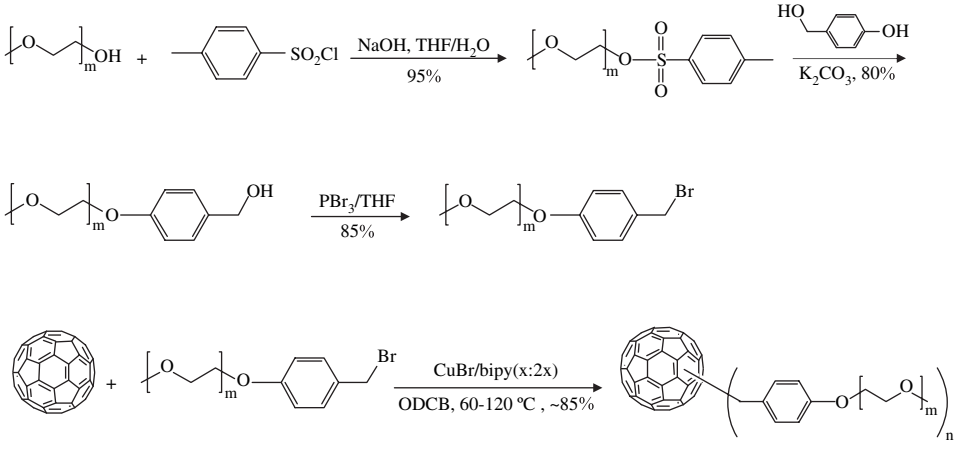

Fig. 1. The synthetic route of poly[tri(ethylene oxide)benzyl]fullerene. In this work, the fullerene derivative with $m = 3$ and $n = 5$ was used.

overnight. The dried Nafion film was dissolved in dimethylacetamide (DMAc). This solution (to be denoted as the Nafion–DMAc solution) was stirred for several hours and cast onto a Teflon substrate. The film was dried at 120 °C overnight, then annealed at 150 °C for an hour and later at 170 °C for half an hour (to be referred to as the recast Nafion). The same annealing process was taken for the composite membranes as well. To fabricate the C_{60}–Nafion composite, a small amount of ODCB was first added to the Nafion–DMAc solution at 80 °C under vigorous stirring. Subsequently, a known amount of C_{60} was dissolved in chlorobenzene (CB), and the C_{60}–CB solution was added to the Nafion–DMAc solution while stirring. The resulting solution was cast onto a Teflon substrate and dried overnight. The casting procedure was the same for other membranes. The amount of C_{60} in Nafion was 1 wt% (the composite to be referred to as C_{60}–Nafion). As to the PHF composite, PHF was first dissolved in DMAc, which was added to the separately prepared Nafion–DMAc solution. The weight percentage of PHF ranged from 1 to 3 (to be referred as PHF–Nafion). Finally, $C_{60}(TEO)_5$ was mixed in another Nafion–DMAc solution at 80 °C, to which ODCB was added and mixed with the C_{60}–CB solution, to fabricate the 1 wt% C_{60}–0.5 wt% $C_{60}(TEO)_5$–Nafion composite. Finally, the membrane was treated by boiling in 1 M H_2SO_4 aqueous solution for 1 h, followed by washing by deionized water.

2.3. Fullerene extraction from Nafion composite membranes

The amount of PHF extracted from the Nafion composite membrane in water was determined to examine the physical stability of the fullerene derivative in the Nafion polymer matrix. First, the PHF/Nafion 117 composite (doped) membrane was dried in a flask by heating at 105 °C under vacuum for 1 h on a sand bath. Then, the flask was purged with nitrogen and the membrane's weight was determined. Subsequently, the membrane was immersed in water at ambient temperature for 120 h, after which the membrane was dried in the same manner as above and the weight was measured. From the weight difference between before and after the immersion in water, the extraction of PHF was determined. As to the extraction from the PHF–Nafion composite (solution cast) membrane, UV–vis spectroscopy was used to quantify the extraction by identifying the peaks characteristics to PHF in the extracted solution of the PHF–Nafion composite. Perkin–Elmer Lambda 20, UV–vis Spectrometer was used.

2.4. Water uptake measurements

The water uptake was measured by soaking the membrane in water at room temperature for 24 h. The membrane was removed from water and blotted gently to remove surface waste, then transferred quickly into a sealed vial and weighed (W_{wet}). The membrane was then vacuum dried at 105 °C overnight, transferred quickly into a sealed vial under dry N_2 protection and weighed (W_{dry}). The *wet* water uptake was determined by the following equation:

$$\text{Wet water uptake} = \frac{(W_{wet} - W_{dry})}{W_{dry}} \quad (1)$$

To measure the water uptake under 25% RH, the membranes were equilibrated under 25% RH for 2 days and weighed afterward as $W_{25\%}$. *Dry* water uptake was estimated from the following equation:

$$\text{Dry water uptake} = \frac{(W_{25\%} - W_{dry})}{W_{dry}} \quad (2)$$

2.5. Thermogravimetric analysis (TGA)

After all samples were equilibrated in water for 24 h, they were blotted on the surface before the measurement. For constant temperature measurements, the weight of the sample was monitored under dry N_2 gas flow of 50 ml min^{-1} at 30 °C for 40 min. For heating measurements, the sample was first subjected to dry N_2 gas for 30 min at a rate of 50 ml min^{-1} prior to heating cycle and gradually heated at the rate of 2 °C min^{-1}. Mettler Toledo TGA/SDTA 851e was used for the TGA measurements.

2.6. ^1H pulse NMR T_2 measurements

The experiments were performed on a Bruker Avance 300 MHz solid state instrument. The membranes were cut to the desired size to fit into the solid state NMR sample holder. Prior to the measurements, the membranes were soaked for 24 h in water and then removed from the water and the surface was blotted. The sample was then placed in the sample holder, which was then placed in the NMR probe. T_2 experiments were run using the Carr–Purcell–Meiboom–Gill pulse sequence [27,28] with a 90° pulse of 4.4 μs at room temperature. Using a 2τ of 100 μs, 92 points on the decay curve were sampled at various evolution times, for the following samples: the recast Nafion, the 1 wt% PHF–Nafion, the 3 wt% PHF–Nafion, and the 1 wt% C_{60}–Nafion composites. Sixteen scans were co-added to improve the signal-to-noise ratio. The data was processed to obtain a plot of signal intensity against evolution time. The data was fit to the equation $M(t) = M(0)\sum P_i(e^{-t/T_{2i}})$, where $M(t)$ and $M(0)$ are the intensity at time t and 0, respectively, P_i is the fraction contributing to the relaxation time T_{2i}, and t the evolution time [29].

2.7. ATR Fourier transform infrared (ATR FT-IR) spectroscopy

ATR FT-IR spectroscopy was employed to investigate the interactions between the fullerene and the Nafion polymer. Measurements were recorded using Nicolet Impact 400 FT-IR spectrometer. After saturation in water overnight, the fullerene composites were dried in an oven at 80 °C for 6 h,

followed by further drying under a vacuum at room temperature for 18 h, prior to the measurements.

2.8. AC impedance measurements

AC impedance of the membranes was determined at 20 °C in the frequency range of 1 to 10^5 Hz using Solartron SI 1260 Impedance Analyzer and SI 1287 Electrochemical Interface. The membranes were subjected to on-plane measurements. The temperature and the relative humidity (RH) of the cell were maintained at 20 °C and under 80%, respectively. The resistance associated with the membrane at zero phase angle was used to estimate the proton conductivity of the membrane using the equation, $\sigma = (1/R)(L/A)$, where R is the bulk resistance of the membrane, L represents the membrane length, and A the cross section area of the membrane. The thickness of the membranes was around 110 μm.

2.9. Limiting current density measurements

The MEA was fabricated by the decal method [30]. The anode catalyst for the methanol oxidation was Pt–Ru (RV 30-30, E-TEK, Inc.) and the cathode catalyst for the hydrogen reduction was Pt black (20 $m^2\,g^{-1}$, Johnson-Matthey). The catalyst ink was prepared by adding 5% Nafion dispersion to the catalyst. The ink composition was 85 wt% Pt–Ru and 15 wt% Nafion for the anode, while that for the cathode was 85 wt% Pt and 15 wt% Nafion. Both the inks were uniformly painted onto two Teflon blanks (2.85 cm^2) to give the desired catalyst loading which was 5 and 0.5 mg cm^{-2} for the anode and the cathode, respectively. During the measurement of the limiting current density, the 1 M methanol solution was fed into the cathode at the rate of 5 mL min^{-1}, while the humidified nitrogen gas to the anode at the rate of 35 mL min^{-1}. The limiting current density of the oxidation of methanol, at the anode, permeating through the membrane was determined voltammetrically [31]. The cell voltage sweeping rate was 10 mA min^{-1}.

2.10. Molecular dynamics simulations

Molecular dynamics (MD) simulations were performed in the gas phase for a C_{60} or PHF molecule in the presence of a single Nafion oligomer having the following structure:

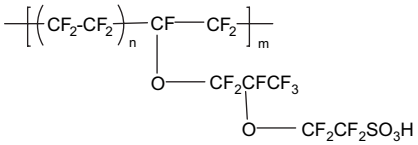

where n and m are 5 and 8, respectively. During the simulations, the hydrogen atoms were kept connected to the sulfonic acid groups of the Nafion chain, since no water was present to dissociate them. The COMPASS force field was used to calculate the potential energy of the system [32]. After equilibration, each simulation was run for 1 ns to collect the data. The electrostatic interactions were treated by the Ewald summation [33]. Bonds with hydrogens were constrained using SHAKE algorithm [34].

3. Results and discussion

3.1. Membrane characterization

It was found that simple mixing of fullerene with commercially available Nafion dispersions, consisting primarily of alcohol and water, only gave a composite membrane with poor dispersion of fullerene (see Fig. 2a). A difficulty of choosing the solvent for solution casting of the fullerene–Nafion composites stems from sharply different solvents available for fullerenes from those for Nafion in general. This circumstance makes fabrication of fullerene–Nafion composites through solution casting difficult, especially when the fullerene is hydrophobic. So far, no co-solvent for hydrophilic fullerenes such as C_{60} and Nafion has been found.

Our search for the solvents was based on the thermodynamic compatibility and the boiling points of the two solvents. With these considerations in mind, ODCB and DMAc have been chosen as our choice for the solution casting of the C_{60}–Nafion composite. ODCB has a high solubility of C_{60}, while DMAc is often used to recast Nafion membranes. Moreover, ODCB and DMAc are completely miscible with one another, while having their b.p. at 180 and at 165 °C, respectively, close enough one another for simple membrane drying

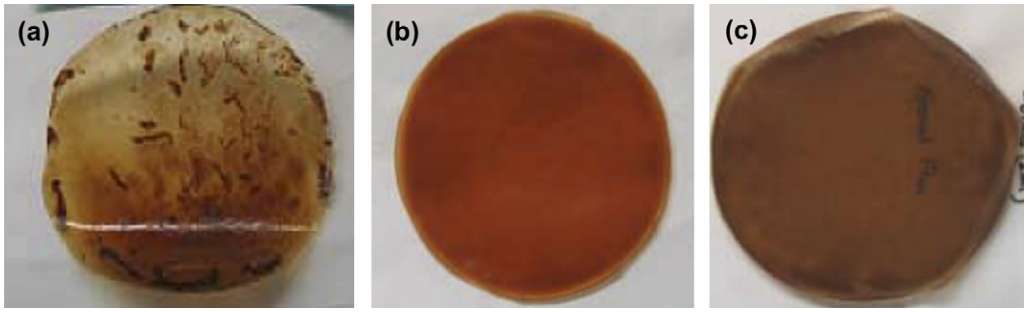

Fig. 2. Photographs of (a) the PHF–Nafion composite film cast from the *iso*-propanol solution (a white line running across the film is an artifact), (b) the PHF–Nafion composite film cast from the DMAc solution, and (c) the C_{60}–Nafion composite film cast from ODCB and DMAc. See text for the details. The loading was 1 wt%.

process. As to the PHF–Nafion composite, since alcohols are in general poor solvents for PHF and DMAc happens to be a good solvent for both PHF and Nafion, DMAc was used as the co-solvent for the solution casting.

Fig. 2 displays the photographs of the solution-cast fullerene–Nafion composite films using ODCB and DMAc, along with the PHF–Nafion composite film prepared by using *iso*-propanol as the main co-solvent for both PHF and Nafion. The loading of the fullerene in the Nafion composite was 1 wt%. The PHF–Nafion film cast out of the *iso*-propanol solution (Fig. 2a) shows a poor dispersion of PHF in the film with a visibly extensive aggregation of PHF. On a sharp contrast, the PHF–Nafion composite prepared by DMAc as the co-solvent (Fig. 2b) displays a much more improved dispersion of the fullerene in the film, as is the case for the C_{60}–Nafion composite (Fig. 2c). The color of the C_{60}–Nafion composite film is dark brown, while that of the PHF–Nafion composite film is reddish brown which is a characteristic of PHF's red shift in the UV–vis spectrum from that of C_{60}.

Fig. 3 illustrates the optical micrograms (OMs) of the doped and solution-cast composites, revealing the dispersion of the fullerenes in more detail. The loading of the fullerene was 1 wt%. The OMs were chosen according to the size of the fullerene agglomerates in the composite membranes. Dramatic differences in the dispersion of the fullerene in the Nafion matrix between the doped and the solution-cast films were apparent. Though the C_{60} agglomerate particles were larger in the solution-cast film than they were in the doped film, the background color was significantly darker than that of the doped film, suggesting a higher concentration of the C_{60} particles in the solution-cast membrane. It is also suspected that some of C_{60} in the doped film may have resided on the film surface after evaporation of the solvent and not all C_{60} molecules may have entered into the Nafion membrane matrix which can be a reason for the lighter color, compared to that of the solution-cast composite. In the doping of C_{60} into a Nafion membrane, toluene was used as the solvent for C_{60}, while methanol was used in the previous work [23]. The larger agglomerates may have been formed during the sedimentation after mixing of the C_{60}–CB solution into the Nafion–DMAc solution. In the PHF–Nafion composites, on the other hand, the agglomerates were much finer and denser than those in the doped film which showed larger, isolated PHF particles. The contrast between the C_{60}–Nafion and the PHF–Nafion composite films reflects the difference in the miscibility of the fullerene in Nafion: C_{60} is highly hydrophobic, thus immiscible in Nafion, while PHF miscible in Nafion.

Fig. 4 displays the OM of the C_{60}–Nafion and PHF–Nafion composites in various loadings. Due to the low miscibility of C_{60} in Nafion, the composite was prepared only up to 1 wt% of C_{60} in Nafion. The size of the C_{60} agglomerate grew and the background color quickly darkened in the C_{60}–Nafion film as the loading increased. On the other hand, a significant change in neither the particle size nor the background color was observed for the PHF–Nafion films up to 1.5 wt%. Even at 1.5 wt% of loading, the PHF composite showed no significant growth of the agglomerate, whereas large agglomerations were observed in the 1 wt% C_{60}–Nafion composite.

In order to examine the effect of the new fullerene dispersant to improve the dispersion of C_{60} in Nafion, $C_{60}(TEO)_5$ was mixed in the C_{60}–Nafion composite. Fig. 5 demonstrates the effectiveness of $C_{60}(TEO)_5$ as a dispersant in the 1 wt% C_{60}–Nafion composite. The OM displays the much smaller C_{60} agglomerate particles having the average agglomerate

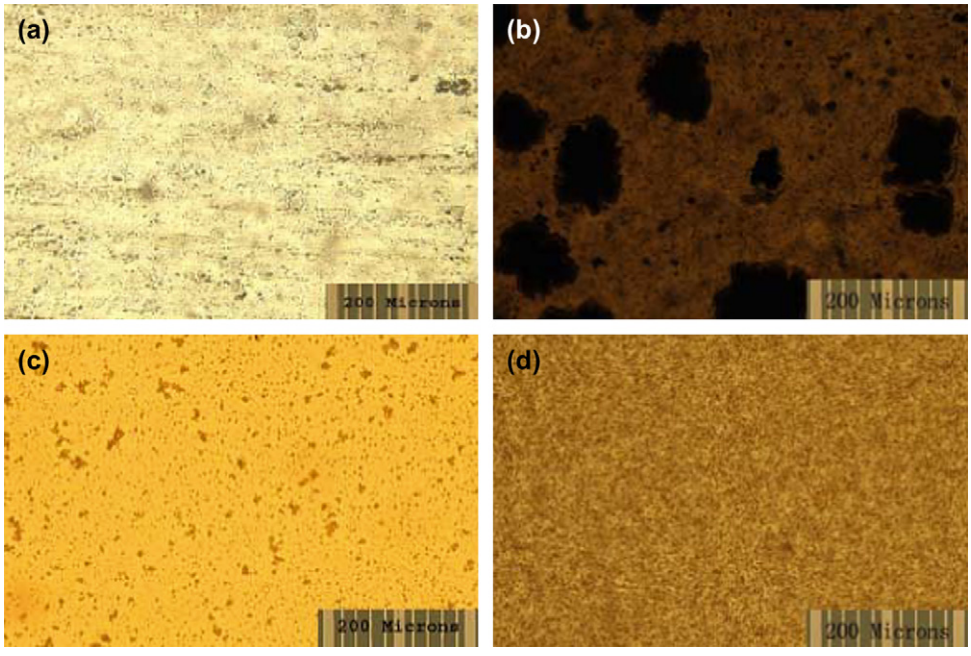

Fig. 3. Optical micrograms of (a) the C_{60}/Nafion 117 and (b) the PHF/Nafion 117 composites by doping, and (c) the C_{60}–Nafion and (d) the PHF–Nafion composites by solution casting. See text for the notations.

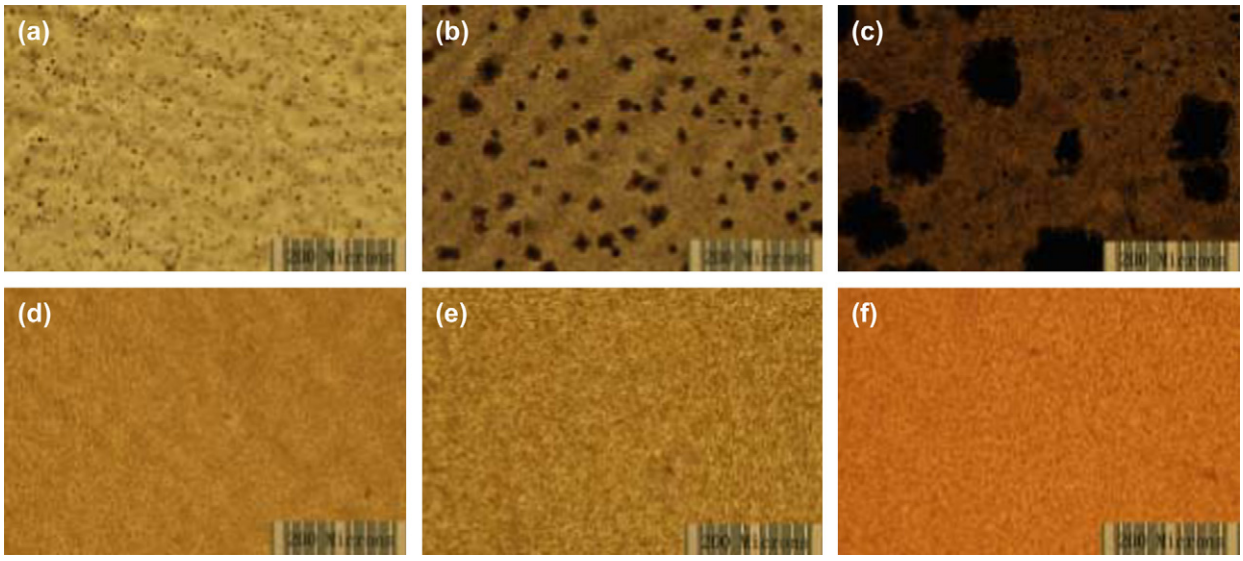

Fig. 4. Optical micrograms of (a) 0.2 wt%, (b) 0.5 wt%, and (c) 1 wt% C_{60}–Nafion and (d) 0.5 wt%, (e) 1.0 wt%, and (f) 1.5 wt% PHF–Nafion composites.

size of approximately 10 μm in diameter, significantly reduced from 100 μm without $C_{60}(TEO)_5$ and the increased dark orange color in the background than that in the absence of $C_{60}(TEO)_5$. This fullerene dispersant should be effective not only to C_{60} but also to other hydrophobic fullerenes. Fig. 6 illustrates the SEM images of the 3 wt% PHF–Nafion composite at different scales. The average particle size is approximately 5 μm in diameter, much smaller than that of the 0.5 wt% C_{60}–Nafion composite.

The physical stability of the fullerene in a Nafion composite film is a concern since it is not chemically attached to the Nafion polymer. The extraction was measured by the membrane weight loss between the dried membrane and the membrane which had been soaked in water at 20 °C for 120 h. Table 1 summarizes the results from the extraction test. For PHF/Nafion 117, the extraction of PHF out of the composite was 65% of the initial amount in the composite membrane. The large loss of PHF is no surprise. In the doped composite, the PHF molecules diffused into the hydrophilic pores of the Nafion membrane which had been swollen by alcohol. Once the composite was soaked in water for the extraction test, the pores may have been opened again and thus PHF was prone to diffusion into water.

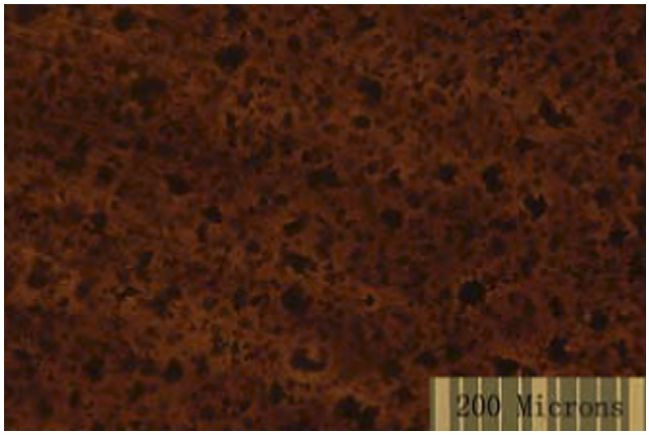

Fig. 5. Optical micrograph of 1 wt% C_{60}–0.5 wt% $C_{60}(TEO)_5$–Nafion composite.

As to the solution-cast PHF–Nafion composite, the amount of extracted PHF was too small to be detected by the weight measurements. Accordingly, UV–vis spectroscopy was employed for the more sensitive determination of PHF in the extracted solution. Separately, a calibration curve was developed to measure the PHF concentration in water from the absorbance in UV–vis spectroscopy. Using the calibration curve, the amount of extracted PHF out of the Nafion composite was determined, as is listed in Table 1. No more than 2.5 wt% of the original PHF was extracted from the composite film, demonstrating a significantly improved stability of PHF in the solution-cast composite, compared to the doped film. In comparison, the extraction of phosphotungstic acid from the Nafion recast composite membrane has also been reported, and the loss of heteropolyacid after immersing the composite membrane in water for 48 h at 30 °C was 24% [35]. Additionally, another PHF–Nafion composite was soaked in boiling water for 2 h and the extracted amount was measured to be less than 1% of the original PHF, showing a favorable stability under the given conditions. Apparently, the solution-cast composite membrane holds the fullerene more tightly than the doped membrane, demonstrating the sharply increased integration of PHF into the Nafion polymer network.

The water characteristics in membranes are important properties for processes such as separation, proton conduction, and others. First, the water uptake was measured both from soaking in water (wet) and under 25% RH (dry). The results are summarized in Table 2 for the 1 wt% C_{60}–Nafion, 3 wt% PHF–Nafion, and the recast Nafion. Apparently, both fullerene composites held more water than the recast Nafion, especially under 25% RH. The higher wet and dry water uptakes of the PHF composites, relative to those of the recast Nafion,

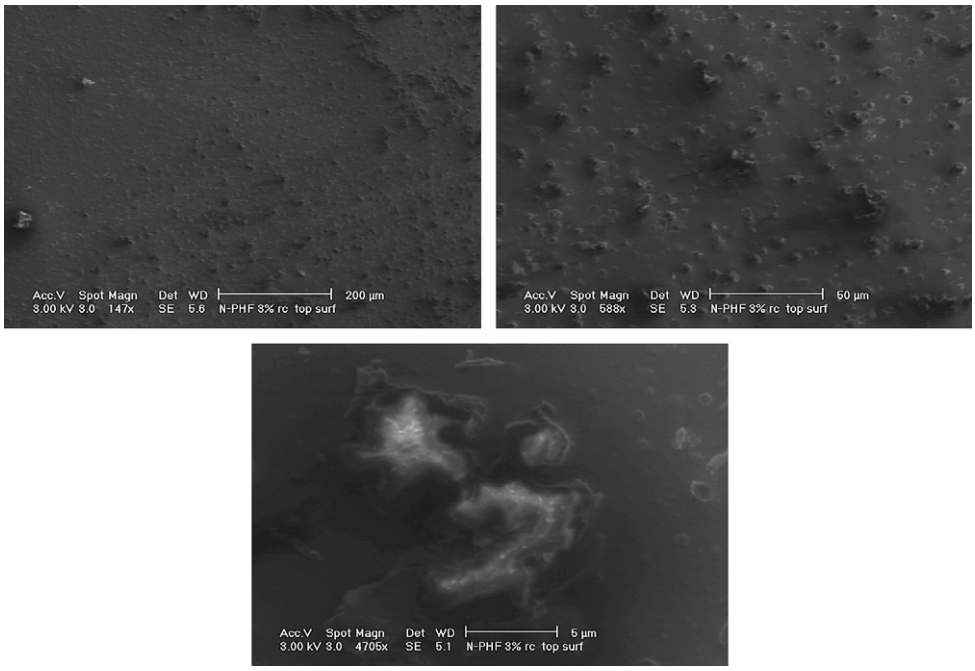

Fig. 6. SEM images of 3 wt% PHF–Nafion at different scales.

were believed to be due to the highly hygroscopic nature of PHF. As to the C_{60} composite, the cause for the higher water uptakes is not clear at this point. There are several possibilities such as the water trapped in the interface between the C_{60} aggregates and the Nafion domain or the morphological change of Nafion caused by the introduction of C_{60} into the Nafion matrix. Due to the small amount of C_{60}, ~1 wt%, no experimental evidence has been found to support either possibility. Only the morphological change by PHF is discussed later.

Next, the water retention in the composites was examined by TGA measurements. The weight loss of the composites was monitored at 30 °C for 40 min, assuming the weight loss under this condition was primarily due to the water loss. Fig. 7(I) displays the weight loss decays of various composite films including the recast Nafion at 30 °C. The weight losses of the same samples during heating up to 250 °C are shown in Fig. 7(II). Both figures indicate considerable differences among the membranes. Table 3 summarizes the water characteristics in each film obtained from the TGA measurements. The data is consistent with the results of the dry water uptake. Under both conditions, the 3 wt% PHF–Nafion composite maintained more water in the membrane than any other membranes studied, suggesting extremely high water retention. The recast Nafion showed the second smallest water loss, while the water remained in the membrane was smaller than others since it had the smallest water uptake to begin with, as shown in Table 2. The 1 wt% C_{60}–Nafion composite lost more water than the 3 wt% PHF–Nafion composites, though it had more wet water uptake than the 3 wt% PHF composite. It is clear that it does not hold water as tightly as the 3 wt% PHF–Nafion composite. Our previous MD simulations have revealed strong interactions between the OH groups of $C_{60}(OH)_{12}$ and the SO_3H groups of Nafion [2]. The sharp difference in the water loss of the 3 wt% PHF composite from any other membranes warrants further study.

T_2 relaxation time determined from ^1H pulse NMR spectroscopy can provide valuable information on the water mobility in the membrane [36,37]. Fig. 8 displays T_2 decays of the fullerene composites including the recast Nafion. Significant differences are observed among the membranes. The slow decay for the 1 wt% C_{60}–Nafion composite suggests the mobile water in the membrane, a manifestation of weaker interactions between water and its surrounding in the C_{60}–Nafion composite. On the other hand, the recast Nafion shows

Table 1
Extraction of PHF out of Nafion composites

	1 wt% PHF/Nafion 117	1 wt% PHF–Nafion	
Extracted PHF,[a] wt%	65[b]	2.5[c]	<1[d]

[a] The weight percentage of the extracted PHF relative to the original amount in the composite.
[b] Determined by weight measurements after soaking in water for 120 h at 20 °C.
[c] Determined by UV–vis spectroscopy after soaking in water for 120 h at 20 °C.
[d] Determined by UV–vis spectroscopy after soaking in boiling water for 2 h.

Table 2
Water uptake for fullerene–Nafion composite membranes (%)

Water uptake	Recast Nafion	1 wt% C_{60}–Nafion	3 wt% PHF–Nafion
Wet[a]	23.87	27.96	26.62
Dry[b]	3.71	5.89	7.96

[a] See Eq. (1).
[b] See Eq. (2).

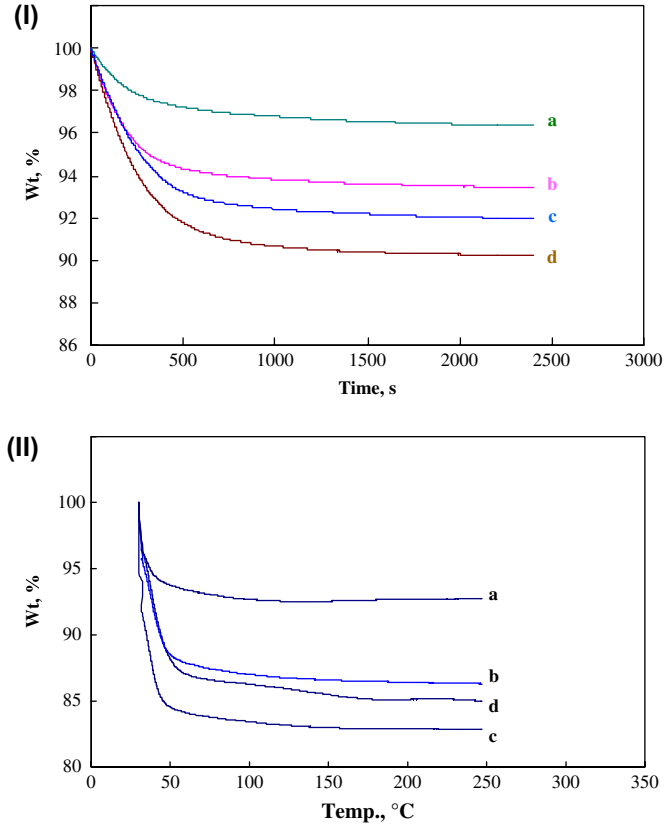

Fig. 7. The weight loss decays of (I) the membranes under dry N_2 gas flow at 30 °C and (II) under dry N_2 gas flow at the heating rate of 2 °C min^{-1} measured by TGA : (a) 3 wt% PHF–Nafion, (b) the recast Nafion, (c) 1 wt% PHF–Nafion, and (d) 1 wt% C_{60}–Nafion.

a very quick decay, indicative of the immobile water, rather unexpected. Our separate DSC measurements confirmed that the recast Nafion had little free water, showing the endothermic heat flow peak due to the melting of ice well below 0 °C. With little free water in the membrane, the water in the recast Nafion can be mostly characterized as bound water, thus the slow decay. This may be a result of the annealing at 170 °C. Lee et al. have found that a recast Nafion annealed at high temperatures had smaller ionic clusters and lower water uptake than those annealed at lower temperatures [38]. Kim et al. have reported similar T_2 results for their membranes having little free water [37]. The water characteristics of the recast Nafion needs further study. The PHF composites exhibit the

Table 3
Water characteristics in the membranes[a]

	Recast Nafion	1 wt% C_{60}–Nafion	1 wt% PHF–Nafion	3 wt% PHF–Nafion
At 30 °C after 40 min				
Water loss, %	6.58	9.79	8.04	3.66
Water remained,[b] %	17.29	18.35	18.35	22.96
At 250 °C with a heating rate of 2 °C min^{-1}				
Water loss, %	13.72	14.12	17.15	7.28
Water remained,[b] %	10.15	13.84	9.24	19.34

[a] From TGA measurements under dry N_2 gas flow.
[b] The amount of water in the membrane after the measurements.

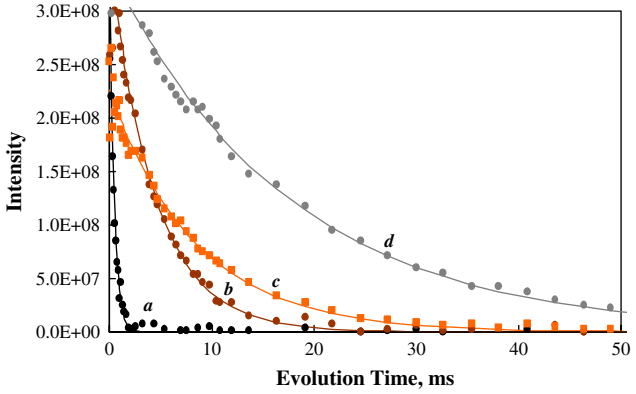

Fig. 8. T_2 decays of (a) the recast Nafion, (b) 3 wt% PHF–Nafion, (c) 1 wt% PHF–Nafion, and (d) 1 wt% C_{60}–Nafion. The dots are the experimental data, while the lines are the calculated data from curve fitting.

decays in between 1 wt% C_{60}–Nafion and the recast Nafion, suggesting the state of the water in those membranes to range from somewhat tightly bound water to loosely bound water. Table 4 includes the T_2 values obtained from curve fitting to the decays.

The location of the fullerene in the Nafion matrix is critical in understanding the composite properties. Yet, probing the location of C_{60} in Nafion was difficult due to the small loading and a rapid growth of aggregation with increasing loading made any change in spectroscopy obscure. Accordingly, we focused on the examination of the location of PHF in the Nafion matrix. Fig. 9 displays the ATR FT-IR spectra for the dry samples of (a) the recast Nafion, (b) 1 wt% PHF–Nafion, and (c) 3 wt% PHF–Nafion in the region for the SO_3^- symmetry stretching, where the largest change was observed upon the addition of PHF to Nafion. Though the 1 wt% PHF composite shows little change, the 3 wt% PHF composite exhibits a clear shift to a lower frequency which suggests interactions between PHF and the SO_3^- group of Nafion, possibly hydrogen-bond like interactions. This change is consistent with the hydrophilic nature of PHF which is likely to reside more in the ionic cluster of the Nafion matrix.

Computer simulations may give valuable insight into the interactions between the fullerene and the Nafion polymer. Detailed analysis requires many samplings of condensed phase simulations including the fullerene located in various domains of the Nafion polymer after adequate simulation time, which demands serious computer resources, beyond the scope of this study. On the other hand, simple MD simulations in the gas phase may give insight into the essential aspect of the fullerene–Nafion interactions. Fig. 10a depicts the initial structure where the Nafion oligomer chain had both backbone and side chains stretched all in *trans* conformation adjacent to which the fullerene was placed.

Table 4
T_2 Values for the fullerene composites including the recast Nafion[a]

	Recast Nafion	1 wt% PHF–Nafion	3 wt% PHF–Nafion	1 wt% C_{60}–Nafion
T_2, μs	0.5	4.4	8.4	17.3

[a] Determined by curve fitting to the plots in Fig. 8.

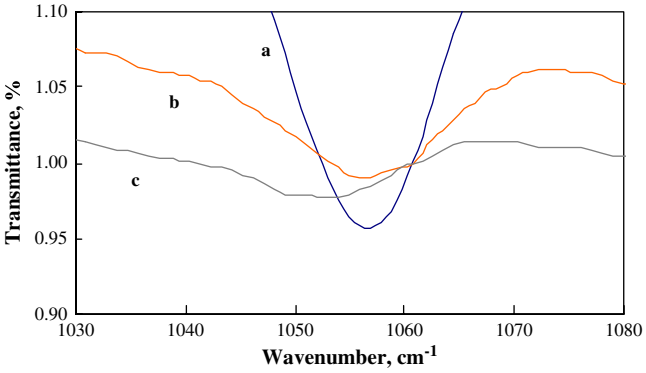

Fig. 9. ART-IR spectra of (a) the recast Nafion, (b) 1 wt% PHF–Nafion and (b) 3 wt% PHF–Nafion. The spectra are expanded for the region due to the SO_3^- symmetry stretching.

First, the Nafion oligomer chain alone was subjected to MD simulations. After 200 ps, the chain transformed itself to a coil with the side chains pointing inside and the backbone outside and largely remained the same as illustrated in Fig. 10b. This conformation ensured the maximum interactions among the hydrophilic side chains. Then, MD simulations of the fullerene–Nafion complex were performed. The initial structure, shown in Fig. 10a, gradually underwent a transition to the fullerene completely wrapped around by the Nafion oligomer after approximately 200 ps for both (C_{60}–Nafion and PHF–Nafion) complexes (Fig. 10c and d, respectively) and stayed unchanged afterward.

Fig. 11 illustrates the history of the radius of gyration for each system. It is of particular interest to note that the radius of gyrations of all three systems converged to more or less the same value, ~10 Å, after 400 ps. This observation suggests that the Nafion oligomer can accommodate either fullerene, C_{60} or PHF, at least partially, in the ionic cluster without much perturbation of its inherent chain dimension. Independent simulations with the fullerene originally placed on the opposite side of the Nafion backbone shown in Fig. 10a, thus, the fullerene facing the hydrophobic domain of the Nafion oligomer, eventually resulted in configurations similar to those in Fig. 10, but the simulations took longer.

The detailed inspection from the trajectories of the simulations of the PHF–Nafion oligomer revealed that the hydroxy groups of PHF and the SO_3H groups of Nafion had close contact within the distances of hydrogen bonds: the oxygen–oxygen distances between PHF and the SO_3H groups of Nafion were within 3 Å. This is consistent with the shift observed in the above ATR FT-IR data. After several independent simulations, it seemed that the Nafion chain tried to accommodate the PHF molecule by having the maximum interactions through the SO_3H groups where all SO_3H groups were more or less occupied by the hydroxy groups of PHF. It is of interest to note that C_{60}, highly hydrophobic, is still surrounded by the Nafion chain with its side chains pointing toward C_{60}. C_{60} is electronically neutral with zero charge on each atom in the force field used for simulations, thus creating no electrostatic repulsions between C_{60} and the Nafion oligomer during the simulations. The interactions were strictly controlled by the van der Waals interactions, attractive in nature. Furthermore, the configuration shown in Fig. 10c not only ensured the maximum contact between C_{60} and the oligomer, but also preserved the Nafion's stable coil conformation (shown in Fig. 10b). The interactions between C_{60} and the CF_2 groups of the side chain, hydrophobic in nature, and the attractive interactions among the side chains pulled the side chains toward C_{60}. Though these interactions may not be as strong as those between PHF and the Nafion side chains, the smaller radius of the C_{60} molecule, approximately 2 Å less than that of a PHF molecule, gave rise to the comparable overall average radius of gyration for both complexes: 9.6 and 9.8 Å, respectively, as shown in Fig. 11. Yet, the C_{60}-side chain interactions created packets between C_{60} and the backbone chain of the Nafion oligomer. These voids may accommodate some water molecules which are trapped in the C_{60}–Nafion complex to increase water uptake, as is shown in Table 2.

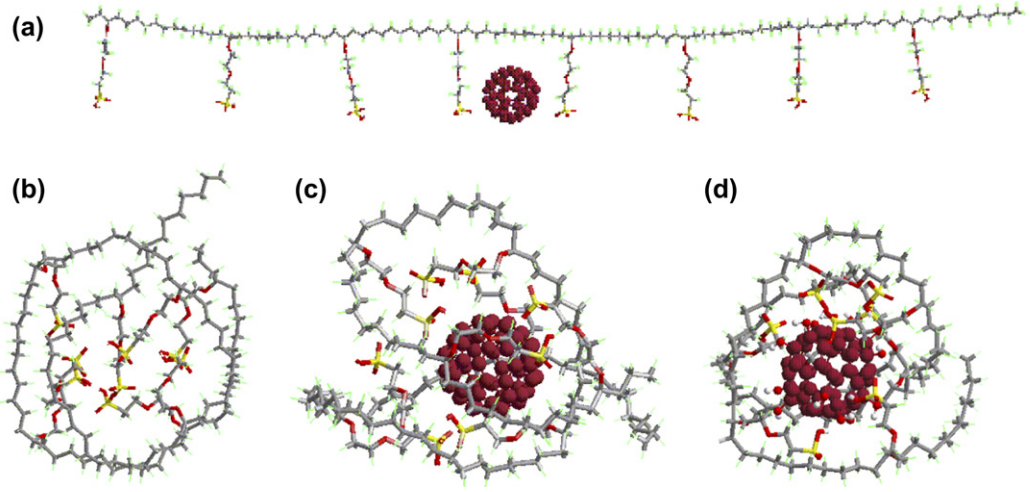

Fig. 10. (a) The initial structure of C_{60} and the Nafion oligomer and the snapshots of (b) the Nafion oligomer, (c) C_{60} and the Nafion oligomer, and (d) PHF and the Nafion oligomer; the last three taken after 1 ns of MD simulations.

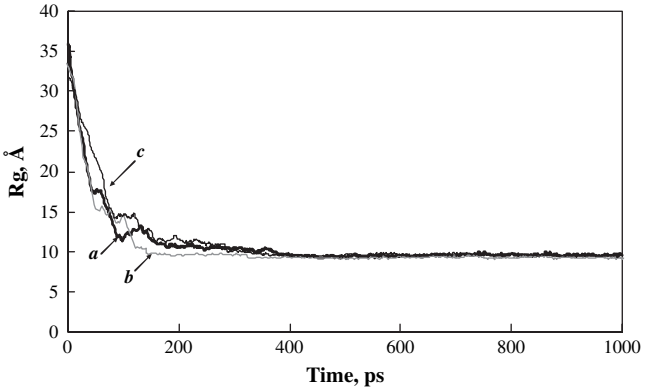

Fig. 11. The radius of gyration of (a) the Nafion oligomer, (b) C_{60} and the Nafion oligomer, and (c) PHF and the Nafion oligomer, as a function of time.

The stabilization energy was calculated from the following equation:

$$\Delta E(\text{fullerene} - \text{Nafion}) = E(\text{fullerene}) - E(\text{Nafion}) - E(\text{fullerene} - \text{Nafion}) \quad (3)$$

where E(fullerene) and E(Nafion) are the potential energies for the fullerene and the Nafion oligomer, respectively, and E(fullerene–Nafion) is the potential energy for the fullerene–Nafion oligomer complex, all in the gas phase. The stabilization energy should be distinguished from the interaction energy between the fullerene and the Nafion oligomer since the conformation of the Nafion oligomer without the fullerene is different from that in the fullerene complex; thus, E(Nafion) is expected to be lower than the energy of the Nafion oligomer in the fullerene complex. The average was taken over the period during which no significant change in the radius of gyration was any longer observed. The calculations indicated that while the stabilization energy for the PHF–Nafion oligomer complex was 58.94 kcal mol^{-1}, that for the C_{60}–Nafion oligomer was only 0.2 kcal mol^{-1}. Clearly, Nafion favorably interacts with PHF due to their hydrophilic nature. As to C_{60}, the result suggests that Nafion can accommodate C_{60} in the hydrophilic domain without much penalty, but the stabilization resulting from the complexation is very small. Since no calculations for the condensed phase were performed, such as the calculations of fullerene sublimation energy, no discussion on the favorable location of the fullerene in the Nafion matrix can be made.

Finally, the limiting current density of the composite membranes was determined voltammetrically. Table 5 summarizes the results. The results for the commercial Nafion membranes, 112, 115 and 117, show a linear relationship between the inverse of the limiting current density and the membrane thickness, as is expected [31]. In fact, the current density normalized by the membrane thickness, $J_{\text{lim}}l$, where l is the membrane thickness, is almost the same for all commercial Nafion membranes. The limiting current density is express as follows:

Table 5
The limiting current density (J_{lim}) of the fullerene composites and Nafion membranes

	J_{lim}, mA cm^{-2}	$J_{\text{lim}}l$[a], mA cm^{-1}
1 wt% C_{60}–Nafion	44.2	0.51
1 wt% PHF–Nafion	40.3	0.47
3 wt% PHF–Nafion	40.0	0.44
Recast Nafion[b]	48.3	0.52
Recast Nafion[c]	30.4	0.52
Nafion 117	37.0	0.68
Nafion 115	54.1	0.68
Nafion 112	125.0	0.69

[a] l is the membrane thickness in centimeter.
[b] $l = 0.0108$ cm.
[c] $l = 0.0171$ cm.

Table 6
The proton conductivity of the fullerene composites and Nafion membranes

	Nafion 117	Recast Nafion	1 wt% C_{60}–Nafion	1 wt% PHF–Nafion	3 wt% PHF–Nafion
σ, $\times 10^{-2}$ S cm^{-1}	4.6	4.4	3.1	3.2	4.6

$$J_{\text{lim}} = 6kFDC/l \quad (4)$$

where k the coefficient, F the Faraday constant, D the methanol diffusion constant, C the methanol concentration, and l the membrane thickness [31]. The limiting current density normalized by l is also listed in Table 5. The fullerene composites all showed lower values for $J_{\text{lim}}l$, relative to the recast Nafion and the commercial Nafion membranes. We assumed the electro-osmotic drag coefficient of the fullerene composites was the same as that of the Nafion membrane, given the small fullerene loading in Nafion, thus the contribution from the convective flow of methanol from the anode to the cathode was likely the same for all the membranes tested. The water characteristics in the fullerene composites discussed above are critical in understanding the limiting current density data of the composites.

It is often observed that inorganic fillers such as SiO_2 and zirconium phosphate can increase the membrane impedance, while reducing the methanol crossover [39,40]. We have measured the proton conductivity of the fullerene composites at room temperature under 80%RH. As is demonstrated in Table 6, the proton conductivity of the fullerene composites is comparable to that of the Nafion membranes; thus the fullerene did not increase the membrane impedance.

4. Conclusion

Both C_{60}–Nafion and PHF–Nafion composite membranes have been successfully fabricated through the solution-cast method for the first time. The fullerene composite membranes exhibited robustness in handling, though thorough mechanical examination needs to be performed for quantitative conclusion. The optical micrograph demonstrated a better integration of the fullerene into the Nafion matrix. Somewhat large agglomerations were still observed in the C_{60}–Nafion composite due to the C_{60}'s poor miscibility in Nafion, while the

PHF–Nafion membrane displayed a uniform dispersion throughout the composite. The dispersion of C_{60} was sharply improved by the new fullerene dispersant, $C_{60}(TEO)_5$, which demonstrated its effectiveness. The physical stability of the PHF composite has been significantly increased from the previously prepared doped membrane, suggesting PHF mostly integrated into the Nafion matrix at a micrometer level. TGA and ^1H pulse NMR measurements have suggested that the fullerene composites have the increased water retention and decreased water mobility, which may be interesting characteristics in light of manipulating the state of water in the membranes.

Based on the results from ATR FT-IR measurement and MD simulations, it is speculated that the PHF molecules can reside in the hydrophilic domain of Nafion while interacting with the SO_3^- groups when the loading is small. The fullerene–Nafion composites prepared in this work should find applications such as fuel cell membranes or optics as suggested earlier [10,19]. The new solution-cast method opens a possibility of direct incorporation of C_{60} into otherwise immiscible polymers without chemical modification of C_{60} which could alter its very unique characteristics. By designing a fullerene dispersant for a given host polymer, the dispersion and the loading of C_{60} can be optimized.

Acknowledgements

The authors wish to thank Professors Wudl and Stucky at University of California at Santa Barbara for the helpful discussions and acknowledge the financial support from DOE (the contract number 21724-001-06).

References

[1] Lichtenberger DL, Nebesny KW, Ray CD, Huffman DR, Lamb LD. Chem Phys Lett 1991;176:203.
[2] Tasaki K, DeSousa R, Wang H, Gasa J, Venkatesan A, Pugazhendhi P, et al. J Membr Sci 2006;281:570.
[3] Lee Y-T, Chiang L-Y, Chen W-J, Hsu H-C. Proc Soc Exp Biol Med 2000;22:69.
[4] Troitskii BB, Troitskaja LS, Yakhnov AS, Lopatin MA, Novikova MA. Eur Polym J 1997;33:1587.
[5] Goswami TH, Nandan B, Alam S, Mathur GN. Polymer 2003;44:3209.
[6] Wang M, Pramoda KP, Goh SH. Chem Mater 2004;16:3452.
[7] Polotskaya GA, Gladchenko SV, Zgonnik VN. J Appl Polym Sci 2002;85:2946.
[8] Jenekhe S, Chen XL. Science 1998;279:1903.
[9] Alivisatos AP. Science 1996;217:933.
[10] Li J, Zhang S, Zhang P, Liu D, Guo Z-X, Ye C, et al. Chem Mater 2003;15:4739.
[11] Wang X, Perzon E, Delgado JL, De la Cruz P, Zhang F, Andersson M, et al. App Phys Lett 2004;85:5081.
[12] Lu J, Dai L, Mau AWH. Acta Polym 1998;49:371.
[13] Sushko ML, Tenhu H, Klenin SI. Polymer 2002;43:2769.
[14] Huang XD, Goh SH. Polymer 2002;43:1417.
[15] Huang XD, Goh SH. Macromolecules 2000;33:8894.
[16] Meier MS. In: Eklund PC, Rao AM, editors. Fullerene polymers and fullerene polymer composites. Berlin: Springer; 1999. p. 369.
[17] Goh HW, Goh SH, Xu GQ, Lee KY, Yang GY, Lee YW, et al. J Phys Chem B 2003;107:6056.
[18] Huang X-D, Goh SH, Lee SY. Macromol Chem Phys 2000;201:2660.
[19] Guo Z-X, Sun N, Li J, Dai L, Zhu D. Langmuir 2002;18:9017.
[20] Eddaoudi H, Deratani A, Tingry S, Sinan F, Seta P. Polym Int 2003;52:1390.
[21] Zhogova KB, Davydov IA, Punin VT, Troitskii BB, Domvachiev GA. Eur Polym J 2005;41:1260.
[22] Zheng J, Goh SH, Lee SY. J Appl Polym Sci 2000;75:1393.
[23] Sun N, Wang Y, Song Y, Guo Z, Dai L, Zhu D. Chem Phys Lett 2001;344:277.
[24] Ouyang J, Pan Y, Zhou S, Goh SH. Polymer 2006;47:6140.
[25] Chiang L-Y, Wang L-Y, Swirczewski JW, Soled S, Cameron S. J Org Chem 1994;59:3960.
[26] Wang H, DeSousa R, Gasa J, Tasaki K, Stucky G, Jousselme B, et al. J Membr Sci 2007;289:277.
[27] Carr HY, Purcell EM. Phys Rev 1954;94:630.
[28] Meiboom S, Gill D. Rev Sci Instrum 1958;29:688.
[29] Gh PY, Hill DJT, Whittaker AK. Biomacromolecules 2002;3:991.
[30] Ren X, Wilson MS, Gottesfeld S. J Electrochem Soc 1996;143:L12.
[31] Ren X, Zawodzinski TA, Springer TE, Gottesfeld S. J Electrochem Soc 2000;147:466.
[32] Sun H. J Phys Chem B 1998;102:7338.
[33] Ewald P. Ann Phys 1918;54:519.
[34] Van Gunsteren WF, Berendsen HJ. Mol Phys 1977;34:1311.
[35] Kim YS, Wang F, Ickner M, Zawodzinski TA, McGrath JE. J Membr Sci 2003;212:263.
[36] Kanekiyo M, Kobayashi M, Ando I, Kurosu H, Ishii T, Amiya S. J Mol Struct 1998;447:49.
[37] Kim YS, Dong L, Hickner MA, Glass TE, Webb V, McGrath JE. Macromolecules 2003;36:6281.
[38] Lee K, Ishihara A, Mitsushima S, Kamiya N, Ota K. J Electrochem Soc 2004;151:A639.
[39] Antonucci PL, Arico AS, Creti P, Rammunni E, Antonucci V. Solid State Ionics 1999;125:431.
[40] Grot WG, Rajendran G. U.S. Patent no. 5,919,583, 1999.